
Performance of ^{11}C -Pittsburgh Compound B PET Binding Potential Images in the Detection of Amyloid Deposits on Equivocal Static Images

Chisa Hosokawa^{1,2}, Kazunari Ishii^{1,3}, Yuichi Kimura⁴, Tomoko Hyodo¹, Makoto Hosono^{1,2}, Kenta Sakaguchi², Kimio Usami², Kenji Shimamoto², Yuzuru Yamazoe², and Takamichi Murakami^{1,2}

¹Department of Radiology, Kinki University Faculty of Medicine, Osakasayama, Osaka, Japan; ²Institute of Advanced Clinical Medicine, Kinki University Faculty of Medicine, Osakasayama, Osaka, Japan; ³Neurocognitive Disorders Center, Kinki University Hospital, Osakasayama, Osaka, Japan; and ⁴Kinki University Faculty of Biology-Oriented Science and Technology, Kinokawa, Wakayama, Japan

The goal of this study was to clarify whether binding potential (BP) images using ^{11}C -Pittsburgh compound B (^{11}C -PiB) and dynamic PET can reliably detect cortical amyloid deposits for patients whose ^{11}C -PiB PET static images are ambiguous and whether visual ratings are affected by white matter retention. **Methods:** Static and BP images were constructed for 85 consecutive patients with cognitive impairment after ^{11}C -PiB dynamic PET. Cortical uptake was visually assessed as positive, negative, or equivocal for both types of images. Quantitatively, the standardized uptake value ratio (SUVr) from the static image, the nondisplaceable BP from the dynamic image for mean gray matter uptake, and the ratio of gray matter uptake to white matter retention were compared among ^{11}C -PiB-positive, ^{11}C -PiB-equivocal, and ^{11}C -PiB-negative groups. **Results:** Forty-three scans were visually assessed as ^{11}C -PiB-positive in both the static and the BP images. Ten scans were ^{11}C -PiB-equivocal in the static images. In 8 of them, the BP images were ^{11}C -PiB-positive, whereas the other 2 were ^{11}C -PiB-equivocal. Thirty-two scans were assessed as ^{11}C -PiB-negative in the static images. In the BP images, 4 were ^{11}C -PiB-positive and 2 were ^{11}C -PiB-equivocal. The mean gray matter uptake of ^{11}C -PiB in SUVr and nondisplaceable BP, respectively, showed statistically significant differences among the ^{11}C -PiB-positive, ^{11}C -PiB-equivocal, and ^{11}C -PiB-negative groups. The ratio of gray matter uptake to white matter retention was lower in the BP images than static images from the ^{11}C -PiB-negative and ^{11}C -PiB-equivocal groups, whereas it was higher in the ^{11}C -PiB-positive group. **Conclusion:** ^{11}C -PiB PET BP images can clarify visual interpretation of clinical static ^{11}C -PiB-equivocal images by reducing the interference of nonspecific white matter retention. We conclude that ^{11}C -PiB-equivocal PET findings on static images reflect cortical amyloid deposits, which can be verified using BP images. Furthermore, quantitative assessments, such as SUVr and nondisplaceable BP, are of no use for correctly rating equivocal visual findings.

Key Words: ^{11}C -PiB; positron emission tomography; binding potential; equivocal; white matter retention

J Nucl Med 2015; 56:1910–1915

DOI: 10.2967/jnumed.115.156414

The amyloid imaging tracer ^{11}C -Pittsburgh compound B (^{11}C -PiB) has been developed for in vivo PET imaging of pathology in Alzheimer disease (AD) (1–3). AD is characterized by the presence of amyloid plaques containing fibrillar amyloid β and neurofibrillary tangles as well as significant loss of neurons in the brain (4–6). ^{11}C -PiB ([*N*-methyl- ^{11}C] 2-(4'-methylaminophenyl)-6-hydroxybenzothiazole) is a thioflavin-T derivative, a small molecule known to bind to amyloid proteins (1), and previous studies have indicated that many patients with AD show cerebral cortical ^{11}C -PiB accumulation; this has been corroborated by pathologic studies (7–9).

Cerebral cortical amyloid deposits are commonly rated as ^{11}C -PiB-positive or ^{11}C -PiB-negative based on uptake assessed by ^{11}C -PiB PET. However, the visual evaluation of static images can result in equivocal ratings (10). Nonspecific white matter ^{11}C -PiB retention is believed to conceal slight cortical uptake (11). Conversely, kinetic model-based approaches with dynamic data for reversibly bound radiotracers, such as ^{11}C -PiB, allow for the quantification of parameters that more directly reflect the binding density, therefore making it easier to detect amyloid deposits. Static images and distribution volume images are considered comparable when using ^{11}C -PiB PET after the patient has achieved an equilibrium state (3).

The goal of the present study was to evaluate the visual interpretation of ^{11}C -PiB-equivocal static images, compared with the visual interpretation of binding potential (BP) images, and to evaluate the effect of white matter retention on rating, regardless of whether cortical uptake is present.

MATERIALS AND METHODS

Patient Population

This retrospective study included 85 patients (38 men and 47 women; mean age \pm SD, 69.2 \pm 10.1 y; mean Mini-Mental State Examination score, 23.4 \pm 5.1) who underwent ^{11}C -PiB dynamic PET

Received Feb. 24, 2015; revision accepted Aug. 31, 2015.
For correspondence or reprints contact: Dr. C. Hosokawa, Department of Radiology, Kinki University Faculty of Medicine, 377-2 Ohnohigashi, Osakasayama, Osaka 589-8511, Japan.
E-mail: ch4111@gmail.com
Published online Sep. 10, 2015.
COPYRIGHT © 2015 by the Society of Nuclear Medicine and Molecular Imaging, Inc.

TABLE 1

Comparison of Visual Assessments of Static and BP Images

Static/BP	Negative	Equivocal	Positive
Negative	26	2	4
Equivocal	0	2	8
Positive	0	0	43

from June 2011 to December 2013. The study included 26 patients with AD, 20 with mild cognitive impairment, 5 with frontotemporal lobar degeneration, 8 with Lewy body disease, and 26 with no clear diagnosis. We used the diagnostic criteria of the Neurologic and Communicative Disorders and Stroke-Alzheimer Disease and Related Disorders Association for AD (12) as well as the third report of the Dementia with Lewy Bodies Consortium for DLB (13). Patients with mild cognitive impairment and frontotemporal lobar degeneration fulfilled the published criteria (14,15). All subjects underwent ^{18}F -FDG PET screening within 1–175 d (mean, 15.2 d; median, 12 d) of ^{11}C -PiB PET scanning. The institutional ethics committee approved this study, and all subjects or guardians signed a written informed consent form.

Data Acquisition

Data acquisition of ^{11}C -PiB PET and ^{18}F -FDG PET was similar to a previous study (10). In brief, PET scans were obtained using a PET scanner (ECAT Accel; Siemens AG) in the 3-dimensional mode. For ^{11}C -PiB PET, data were continuously acquired for 70 min after intravenous administration of 555 ± 185 MBq of ^{11}C -PiB. For ^{18}F -FDG PET, a 30-min emission scan was acquired, starting 30 min

TABLE 2

Comparison of Visual White Matter Uptake Between Static and BP Images Among 3 Static Rating Groups

Group	Negative	Equivocal	Positive
Static > BP	23	9	34
Static = BP	9	1	9
Static < BP	0	0	0

after intravenous injection of 185 MBq of ^{18}F -FDG. This acquisition was solely for the purpose of assisting registration of the other images.

Image Processing

Static images of the ^{11}C -PiB PET scans consisted of the sum of four 5-min frames from 50 to 70 min. For BP images, data analyses were done with the PMOD software package (version 3.308; PMOD Technologies Ltd.) using the full set of dynamic data (0–70 min after injection) as follows: parametric images of regional ^{11}C -PiB uptake (i.e., BP images) were generated using Logan graphical analysis, which referenced the cerebellar cortex (16).

Spatial normalization was performed as follows. Each static and BP image was coregistered with the corresponding ^{18}F -FDG PET image using SPM8 (Wellcome Department of Imaging Neuroscience). First, spatial normalization of the ^{18}F -FDG PET images to the Montreal Neurologic Institute space was performed using the SPM8 program. Next, spatial normalization of the coregistered static and BP images to the Montreal Neurologic Institute space was performed using the individual parameters obtained from ^{18}F -FDG PET normalization.

TABLE 3

Demographics and Results of 10 ^{11}C -PiB-Equivocal and 6 ^{11}C -PiB-Negative Subjects

Age	Sex	Diagnosis	MMSE	Visual assessment				Quantification		
				Static	sn-SUVR – 1	BP	sn-BP	White matter	SUVR	BP _{ND}
74	Female	UD	23	N	N	E	E	Static = BP	1.01	0.39
54	Male	UD	29	N	N	E	E	Static = BP	0.98	0.26
83	Male	AD	25	N	N	P	P	Static > BP	1.07	0.06
66	Male	UD	28	N	N	P	P	Static > BP	1.17	0.04
62	Male	MCI	—	N	N	P	P	Static > BP	1.02	0.2
84	Female	AD	21	N	N	P	P	Static > BP	1.11	0.04
72	Female	AD	22	E	E	E	E	Static = BP	1.35	0.87
75	Female	FTLD	19	E	E	E	E	Static > BP	1.05	0.08
77	Female	UD	24	E	E	P	P	Static > BP	1.37	0.52
81	Male	AD	24	E	E	P	P	Static > BP	1.85	0.62
67	Male	AD	21	E	E	P	P	Static > BP	1.69	0.44
80	Male	MCI	26	E	E	P	P	Static > BP	1.50	0.06
83	Male	MCI	27	E	E	P	P	Static = BP	1.76	0.48
75	Male	PD	20	E	E	P	P	Static > BP	1.38	0.07
79	Male	MCI	25	E	E	P	P	Static > BP	1.61	0.25

MMSE = mini mental state examination; sn = spatially normalized; UD = undiagnosed; N = negative; E = equivocal; P = positive; MCI = mild cognitive impairment; FTLD = frontotemporal lobar degeneration; PD = Parkinson disease.

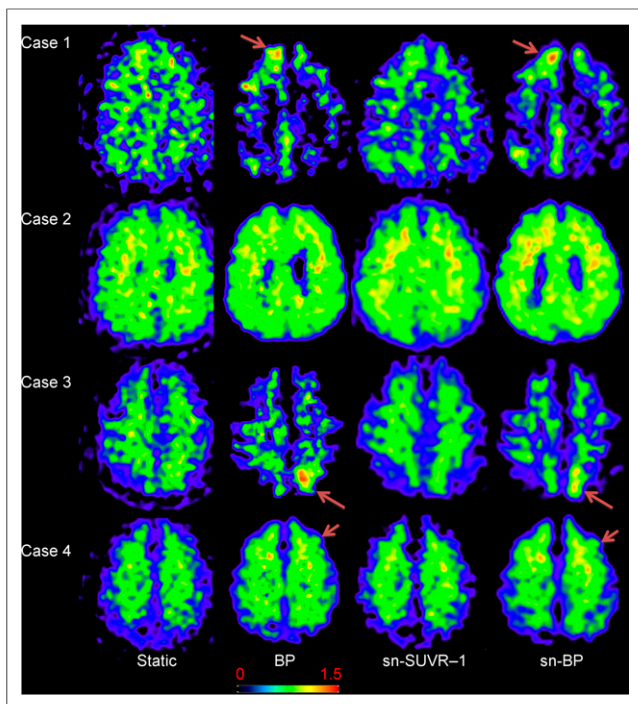


FIGURE 1. Representative images of subjects with ^{11}C -PiB-different ratings in static, BP, sn-SUVR – 1, and sn-BP images. Case 1 is an 80-y-old man: mild cognitive impairment, SUVR-equivocal, and BP-positive. Case 2 is a 72-y-old woman: AD, SUVR- and BP-equivocal. Case 3 is an 83-y-old man: AD, SUVR-negative and BP-positive. Case 4 is a 74-y-old woman, undiagnosed, SUVR-negative and BP-equivocal. SUVR, BP, sn-SUVR – 1, and sn-BP images are demonstrated in order from left to right. Arrows in cases 1 and 3 show ^{11}C -PiB-positive regions, and those in case 4 show ^{11}C -PiB-equivocal portions. In case 2, extended cortical uptake is suspected.

Image Analysis

The ^{11}C -PiB PET static image and the BP image of all scans were visually assessed by 2 experienced nuclear medicine physicians masked to clinical information (10). In brief, each image was classified as ^{11}C -PiB-positive, ^{11}C -PiB-equivocal, or ^{11}C -PiB-negative. When cortical accumulation was suspected, but cortical accumulation was not greater than in the cerebral white matter (from directly beneath cortex to periventricular region), an equivocal rating was assigned. Any level of ^{11}C -PiB uptake in the white matter was identified as ^{11}C -PiB-negative. In addition, we visually examined whether the static or BP image had more white matter uptake. The degree of gray/white matter contrast was compared between the static and the BP image if the assessment was ^{11}C -PiB-positive or ^{11}C -PiB-equivocal; the length of ^{11}C -PiB accumulation from the periventricular area was compared between the static and the BP image if the assessment was ^{11}C -PiB-negative.

An automated quantitative analysis was performed as follows. Standardized uptake value ratios (SUVRs) (referenced to the cerebellar cortex) and nondisplaceable BP (BP_{ND}) were measured using the template volumes of interest (frontal, parietotemporal, precuneus/posterior cingulate, striatum, cerebral white matter, and cerebellar cortex) set in the Montreal Neurologic Institute space. Then, we calculated the mean gray matter SUVR and BP_{ND} from the 4 gray matter values. In addition, the ratio of mean gray matter uptake to white matter retention (R-G/WM) of ^{11}C -PiB was calculated to provide a quantitative measure of whether or not nonspecific white matter retention affected the visual ratings.

Furthermore, for other visual and quantitative assessments, because BP_{ND} is equal to the distribution volume ratio (DVR) minus a value of 1, as described by Innis et al. (17), we obtained spatially normalized SUVR minus 1 (sn-SUVR – 1) images considered to be equivalent to BP images as in the method of Klumpers et al. (18) and calculated DVR ($\text{BP}_{\text{ND}} + 1$).

We visually compared not only the static and BP images, but also the sn-SUVR – 1 images and spatially normalized BP (sn-BP) images of individual ^{11}C -PiB PET. Quantitatively, mean gray matter uptake and the R-G/WM of SUVR, BP_{ND} , and DVR were compared.

We investigated the effect of nonspecific white matter retention on the visual rating and discussed the true interpretation of ^{11}C -PiB-equivocal static images.

Statistical Analysis

Data are presented as mean \pm SD unless otherwise stated. The associations between SUVR and BP_{ND} were analyzed using the Pearson correlation coefficient test. One-way ANOVA and the post hoc Tukey–Kramer test were used to assess differences in SUVR, BP_{ND} , and DVR values among the ^{11}C -PiB-positive, ^{11}C -PiB-equivocal, and ^{11}C -PiB-negative groups. A *P* value of less than 0.05 was considered statistically significant.

RESULTS

The results of visual assessments of ^{11}C -PiB PET static and BP images are shown in Table 1. Ten subjects were visually assessed as ^{11}C -PiB-equivocal from the static image; 8 of 10 were visually rated as ^{11}C -PiB-positive from the BP image. Of 32 ^{11}C -PiB-negative subjects from the static image, 4 were evaluated as ^{11}C -PiB-positive and 2 as ^{11}C -PiB-equivocal from the BP image. The visual ratings of sn-SUVR – 1 and sn-BP images were the same as the static and BP images, respectively. Regarding visual white matter uptake analysis, 66 scans showed a higher uptake in the static image than in the BP image, and 19 scans showed an equivalent uptake. No scans showed higher white matter uptake in the BP image than in the static image (Table 2). Of 10 subjects whose static PiB rating was equivocal, 9 showed higher white matter uptake in the static image than in the BP image.

The demographics and results of visual and quantitative assessments of 10 ^{11}C -PiB-equivocal subjects and 6 static-negative and BP-nonnegative subjects are shown in Table 3. In 8 static ^{11}C -PiB-equivocal and BP ^{11}C -PiB-positive subjects, 7 visually showed lower white matter uptake in BP images than static images. All 4 static ^{11}C -PiB-negative and BP ^{11}C -PiB-positive subjects also showed lower white matter uptake in the BP images. Three of 4 BP ^{11}C -PiB-equivocal subjects showed equivalent white matter uptake in both static and BP images. Representative images are provided in Figure 1. White matter uptake was visually less in BP and sn-BP images than in static and sn-SUVR images (Fig. 1, cases 1 and 3), resulting in easier detection of cortical uptake on BP and sn-BP images. In contrast, cortical uptake was difficult to detect when white matter uptake was equivalent in static and BP images or in sn-SUVR images and sn-BP images (Fig. 1, cases 2 and 4).

According to quantitative analyses, a significant correlation was observed between SUVR and BP_{ND} for the ^{11}C -PiB PET scans (Fig. 2). There were no negative results for BP_{ND} in this investigation. For ^{11}C -PiB-negative, ^{11}C -PiB-equivocal, and ^{11}C -PiB-positive groups, mean gray matter SUVR was 1.02 ± 0.07 , 1.50 ± 0.24 , and 2.11 ± 0.34 , whereas BP_{ND} was 0.10 ± 0.09 , 0.38 ± 0.27 , and 0.44 ± 0.37 , respectively, with statistically significant differences ($P < 0.01$) among the 3 groups (Fig. 3). Although both mean gray matter SUVR and BP_{ND} of the ^{11}C -PiB-equivocal

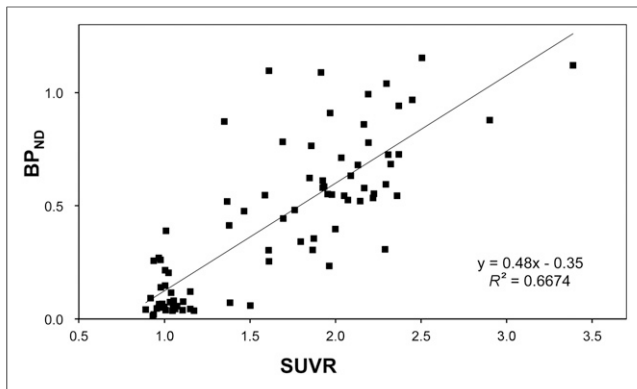


FIGURE 2. Correlation between mean gray matter SUVR and BP_{ND} in all subjects.

group were intermediate between values from the ¹¹C-PiB-negative and ¹¹C-PiB-positive groups, the range of ¹¹C-PiB-equivocal values overlapped with the ¹¹C-PiB-negative and ¹¹C-PiB-positive groups, especially for BP_{ND}.

The R-G/WM of SUVR, BP_{ND}, and DVR values calculated for the 3 groups are shown in Figure 4.

Of the 3 metrics, BP_{ND} showed the largest contrast of R-G/WM between ¹¹C-PiB-negative and ¹¹C-PiB-positive groups. In the static ¹¹C-PiB-positive group, mean R-G/WM was 0.96 in SUVR and 1.07 in DVR, whereas it was 1.20 in BP_{ND}. Likewise, in the static ¹¹C-PiB-negative group, mean R-G/WM was 0.56 in SUVR and 0.81 in DVR, whereas it was 0.28 in BP_{ND}. The R-G/WM of SUVR was higher than the BP_{ND} in the ¹¹C-PiB-negative and ¹¹C-PiB-equivocal groups and lower in the ¹¹C-PiB-positive group. DVR showed the least differences among the 3 groups.

DISCUSSION

Our investigation revealed 4 interesting findings. First, we showed that BP images were visually more sensitive than static images for the detection of cortical ¹¹C-PiB uptake in ¹¹C-PiB static images visually assessed as equivocal. It is sometimes difficult to visually make dichotomized classifications of ¹¹C-PiB PET findings (10). Assessments of in vivo ¹¹C-PiB PET for cortical amyloid deposits have been performed using the distribution

volume or DVR with dynamic data, and Price et al. (3) reported that the Logan graphical analysis was practical and reliable. However, ¹¹C-PiB PET static images have been commonly used for clinical purposes, because they do not require dynamic scans and blood sampling. The DVR in PET is defined as the ligand concentration ratio of target tissue and blood at equilibrium, and static images are obtained at equilibrium after radiotracer administration. Therefore, static images and DVR images are considered comparable (19). The BP reflects the receptor concentration and ligand affinity for receptors in the target tissue (20), and BP_{ND} is DVR - 1 (3,17-19). Generally, DVR images, not BP images, have been used, because BP_{ND} analyses may produce negative values (3,19). The present study compared BP images generated using the Logan graphical analysis with static images. Because static images and BP images produce different results, we compared sn-SUVR - 1 images with sn-BP images. Although sn-SUVR - 1 and sn-BP images are scored as equivalent, ratings of sn-SUVR - 1 were the same as static images. In other words, sn-SUVR - 1 images were not able to detect cortical uptake, whereas sn-BP images could. These results indicate that static and dynamic parametric images are essentially different. Comparisons between static and BP images produced the same visual findings as those between sn-SUVR - 1 and sn-BP images. Therefore, we consider that comparisons between static images and BP images are possible. Zwan et al. compared SUVR images with BP images to determine the optimal approach for visual assessment of ¹¹C-PiB PET; they concluded that BP images were the method of choice for detecting cortical amyloid deposition, because an excellent inter-interpretor agreement was obtained in BP images compared with SUVR images (21). This fact suggests that it is easier to rate cortical ¹¹C-PiB uptake on BP images than on static images. Tracer kinetic analysis can remove nonspecific binding that occurs to sites other than amyloid β, for example, membranes and lipid fractions, metabolites, or vascular activity. Subsequently, parameters, such as DVR or BP_{ND}, can be estimated (22). In the present study, ¹¹C-PiB binding to amyloid β is more precise in BP images than in static images. Therefore, we found that BP imaging reduced the rate of static ¹¹C-PiB-equivocal (12%) to 5%.

Second, quantitative assessments, such as SUVR and BP_{ND}, were found to be of no use for correctly rating equivocal visual findings. The fact that there was overlap in the ranges of quantitative values for the 3 groups demonstrated that quantification was not helpful

for interpreting ¹¹C-PiB-equivocal findings, despite the fact that differences were statistically significant among the 3 groups. In other words, focal or slight cortical ¹¹C-PiB uptake showed low quantitative values in the ¹¹C-PiB-equivocal or ¹¹C-PiB-positive groups. Therefore, visual assessments can detect amyloid β earlier than quantitative analyses, as described by Cohen et al. when they compared visual findings with quantitative analysis of ¹¹C-PiB PET in healthy controls (23).

Third, white matter retention was visually assessed to be greater in static images than in BP images. This demonstrates that lower white matter uptake allows for more sensitive detection of cortical uptake in BP images—that is, the changes of assessments

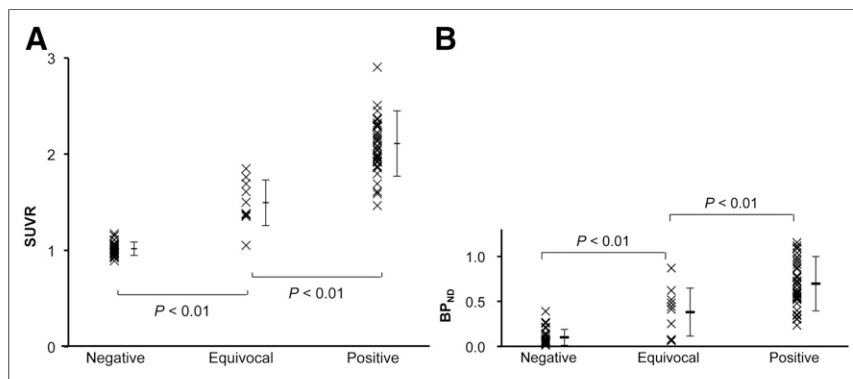


FIGURE 3. Distribution and values of mean gray matter uptake among ¹¹C-PiB-negative, ¹¹C-PiB-equivocal, and ¹¹C-PiB-positive groups (SUVR [A], BP_{ND} [B]).

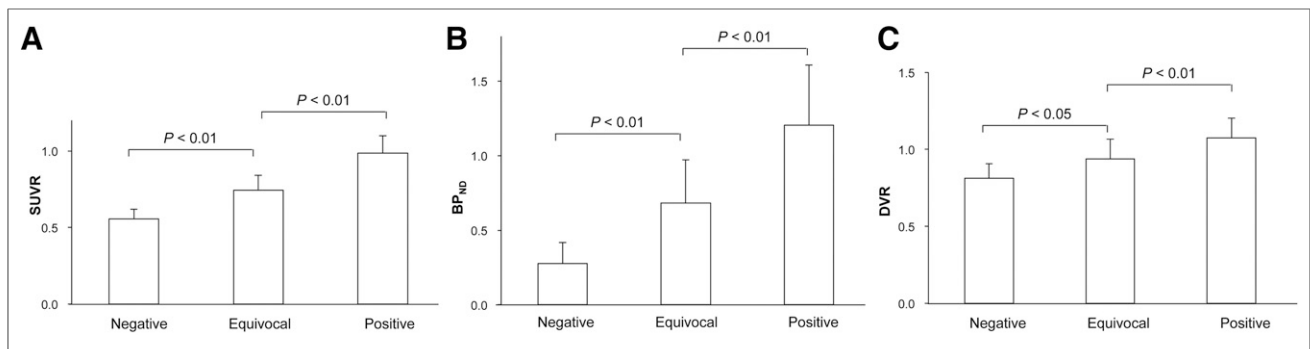


FIGURE 4. Ratio of gray matter ^{11}C -PiB uptake to white matter retention in SUVR (A), BP_{ND} (B), and DVR (C) among ^{11}C -PiB–negative, ^{11}C -PiB–equivocal, and ^{11}C -PiB–positive groups.

are related to the degree of retention of white matter. The image difference between SUVR and BP_{ND} depends on the reference regions. Thus, these results might change depending on the characteristics of participants. We suppose that the detectability of cortical ^{11}C -PiB uptake is visually affected by nonspecific white matter retention (11).

Finally, the ratio of gray matter uptake to white matter retention showed the greatest differences between the ^{11}C -PiB–negative group and the ^{11}C -PiB–positive group in BP_{ND} among the 3 metrics—SUVR, BP_{ND}, and DVR. This result indicates that visual assessment of a BP image can detect cortical uptake more sensitively than SUVR. In our opinion, these results suggest that BP images detect cortical uptake with more sensitivity than true DVR images. In addition, this finding supports the visual finding of lower nonspecific white matter retention in BP images.

On microscopic examination, no amyloid β deposits are found in white matter (5,11). The exact cause of nonspecific white matter binding of amyloid β tracers, such as ^{11}C -PiB PET, is not known. It has been suggested that binding is largely attributable to slower clearance in white matter due to less blood flow, compared with cortical blood flow (11). Conversely, the reason why white matter binding in BP images is lower than in static images remains unclear. We hypothesized that dynamic data acquisition, starting immediately after radiotracer injection along with appropriate analysis, accounts for more factors, such as slow flow, clearance, and lipophilicity, than static imaging that is acquired at the time of equilibrium.

It has been expected that ^{18}F -labeled amyloid tracers would become widely available to allow for acquisition of SUVR images for clinical use (24–28). However, these tracers, other than ^{18}F -AZD4694, show lower cortical-to-white matter contrast than ^{11}C -PiB PET as well as higher white matter binding, which may increase reading difficulty. Therefore, for these tracers, we suggest that visual assessment of cortical uptake using BP images might be more efficient and more accurate than the visual assessment of static images. As a side note, we point out that the data acquisition time is shorter with ^{18}F -florbetapir and ^{18}F -ADZ4694 than with ^{11}C -PiB (26–28).

Our study has some limitations. First, there was no pathologic material for correlation. Therefore, we were not able to compare the ^{11}C -PiB PET findings with AD pathology to determine sensitivity, specificity, and accuracy of the images. Our finding shows that BP_{ND} sensitivity is better. However, because we do not have a gold standard (histologically proven cases), we cannot show the higher specificity of BP_{ND}.

Second, because subjects included various patients with or without AD as part of this retrospective study, the results of this research may not reflect pure AD-related amyloid pathology, because amyloid deposits occur in subjects with cerebral amyloid angiopathy (29) and Lewy body disease (30,31) and in cognitively intact subjects (32). Third, because of the small sample size, we were not able to refer to the relationship between visual ^{11}C -PiB–equivocal ratings and quantitative values, ^{11}C -PiB–equivocal and clinical findings including Mini-Mental State Examination, and that of small cortical amyloid deposits and noncognitive older subjects. Fourth, BP_{ND} had a wide variation relative to SUVR. We suggest further research to address these limitations.

Finally, in the case of the 2 static ^{11}C -PiB–equivocal scans unsolved by BP analysis, we are unsure what should be done. Perhaps additional research, such as other kinetic analyses or repeated scans, would assist in the diagnosis.

CONCLUSION

Although BP analyses have a higher detection rate of cortical ^{11}C -PiB uptake than static images, these analyses are not practical in clinical situations. Our study demonstrates that most ^{11}C -PiB–equivocal findings on static images show as ^{11}C -PiB–positive on BP images. Therefore, we argue that ^{11}C -PiB–equivocal findings in static images could be considered as ^{11}C -PiB–positive. Furthermore, importantly, we found that quantitative assessments, such as SUVR and BP_{ND}, were not helpful for correctly rating equivocal visual findings.

DISCLOSURE

The costs of publication of this article were defrayed in part by the payment of page charges. Therefore, and solely to indicate this fact, this article is hereby marked “advertisement” in accordance with 18 USC section 1734. This study was supported in part by JSPS KAKENHI grant 50534103 and the 21st Century Research and Development Incentive Wages at Kinki University. No other potential conflicts of interest relevant to this article are reported.

ACKNOWLEDGMENT

We thank Yoshiyuki Nakayama for his support for brain ^{18}F -FDG PET and ^{11}C -PiB PET at Kinki University Hospital.

REFERENCES

- Mathis CA, Wang Y, Holt DP, Huang GF, Debnath ML, Klunk WE. Synthesis and evaluation of ^{11}C labeled 6-substituted 2-arylbenzothiazoles as amyloid imaging agents. *J Med Chem*. 2003;46:2740–2754.
- Klunk WE, Engler H, Nordberg A, et al. Imaging brain amyloid in Alzheimer's disease with Pittsburgh compound-B. *Ann Neurol*. 2004;55:306–319.
- Price JC, Klunk WE, Lopresti BJ, et al. Kinetic modeling of amyloid binding in humans using PET imaging and Pittsburgh compound B. *J Cereb Blood Flow Metab*. 2005;25:1528–1547.
- Price JL, Morris JC. Tangles and plaques in nondemented aging and 'preclinical' Alzheimer's disease. *Ann Neurol*. 1999;45:358–368.
- Braak H, Braak E. Neuropathological staging of Alzheimer-related changes. *Acta Neuropathol (Berl)*. 1991;82:239–259.
- Mirra SS, Heyman A, McKeel D, et al. The consortium to establish a registry for Alzheimer's disease (CERAD): part II—standardization of the neuropathologic assessment of Alzheimer's disease. *Neurology*. 1991;41:479–486.
- Ikonomic MD, Klunk WE, Abrahamson EE, et al. Postmortem correlates of in vivo PiB-PET amyloid imaging in a typical case of Alzheimer's disease. *Brain*. 2008;131:1630–1645.
- Kadir A, Marutle A, Gonzalez D, et al. Positron emission tomography imaging and clinical progression in relation to molecular pathology in the first Pittsburgh compound B positron emission tomography patient with Alzheimer's disease. *Brain*. 2011;134:301–317.
- Leinonen V, Alafuzoff I, Aalto S, et al. Assessment of β -amyloid in a frontal cortical brain biopsy specimen and by positron emission tomography with carbon 11-labeled Pittsburgh compound B. *Arch Neurol*. 2008;65:1304–1309.
- Hosokawa C, Ishii K, Hyodo T, et al. Investigation of ^{11}C -PiB equivocal PET findings. *Ann Nucl Med*. 2015;29:164–169.
- Fodero-Tavoletti MT, Rowe CC, McLean CA, et al. Characterization of PiB binding to white matter in Alzheimer disease and other dementias. *J Nucl Med*. 2009;50:198–204.
- McKhann G, Drachman D, Foistein M, Katzman R, Price D, Stadlan EM. Clinical diagnosis of Alzheimer's disease: report of the NINCDS-ADRDA Work Group under the auspices of Department of Health and Human Services Task Force on Alzheimer's disease. *Neurology*. 1984;34:939–944.
- McKeith IG, Dickson DW, Lowe J, et al. Diagnosis and management of dementia with Lewy bodies: third report of the DLB consortium. *Neurology*. 2005;65:1863–1872.
- Petersen RC, Doody R, Kurz A, et al. Current concepts in mild cognitive impairment. *Arch Neurol*. 2001;58:1985–1992.
- Neary D, Snowden JS, Gustafson L, et al. Frontotemporal lobar degeneration: a consensus on clinical diagnostic criteria. *Neurology*. 1998;51:1546–1554.
- Logan J, Fowler JS, Volkow ND, Wang GJ, Ding YS, Alexoff DL. Distribution volume ratios without blood sampling from graphical analysis of PET data. *J Cereb Blood Flow Metab*. 1996;16:834–840.
- Innis RB, Cunningham VJ, Delforge J, et al. Consensus nomenclature for in vivo imaging of reversibly binding radioligands. *J Cereb Flow Metab*. 2007;27:1533–1539.
- Klumpers UM, Boellaard R, Veltman DJ, et al. Parametric [^{11}C]flumazenil images. *Nucl Med Commun*. 2012;33:422–430.
- Lopresti BJ, Klunk WE, Mathis CA, et al. Simplified quantification of Pittsburgh compound B amyloid imaging PET studies: a comparative analysis. *J Nucl Med*. 2005;46:1959–1972.
- Mintun MA, Raichle ME, Kilbourn MR, Wooten GF, Welch MJ. A quantitative model for the in vivo assessment of drug binding sites with positron emission tomography. *Ann Neurol*. 1984;15:217–227.
- Zwan MD, Ossenkoppele R, Tolboom N, et al. Comparison of simplified parametric methods for visual interpretation of ^{11}C -Pittsburgh compound-B PET images. *J Nucl Med*. 2014;55:1305–1307.
- Edison P, Hinz R, Brooks DJ. Technical aspects of amyloid imaging for Alzheimer's disease. *Alzheimers Res Ther*. 2011;3:25–32.
- Cohen AD, Mowrey W, Weissfeld LA, et al. Classification of amyloid-positivity in controls: comparison of visual read and quantitative approaches. *Neuroimage*. 2013;71:207–215.
- Vandenberghe R, Van Laere K, Ivanoiu A, et al. ^{18}F -flutemetamol amyloid imaging in Alzheimer disease and mild cognitive impairment: a phase 2 trial. *Ann Neurol*. 2010;68:319–329.
- Villemagne VL, Ong K, Mulligan RS, et al. Amyloid imaging with ^{18}F -florbetaben in Alzheimer disease and other dementias. *J Nucl Med*. 2011;52:1210–1217.
- Wong DF, Rosenberg PB, Zhou Y, et al. In vivo imaging of amyloid deposition in Alzheimer disease using the radioligand ^{18}F -AV-45 (florbetapir F-18). *J Nucl Med*. 2010;51:913–920.
- Clark CM, Schneider JA, Bedell BJ, et al. Use of florbetapir-PET for imaging β -amyloid pathology. *JAMA*. 2011;305:275–283.
- Rowe CC, Pejoska S, Mulligan RS, et al. Head-to head comparison of ^{11}C -PiB and ^{18}F -AZD4694 (NAV4694) for β -amyloid imaging in aging and dementia. *J Nucl Med*. 2013;54:880–886.
- Johnson KA, Gregas M, Becker JA, et al. Imaging of amyloid burden and distribution in cerebral amyloid angiopathy. *Ann Neurol*. 2007;62:229–234.
- Gomperts SN, Rentz DM, Moran E, et al. Imaging amyloid deposition in Lewy body diseases. *Neurology*. 2008;71:903–910.
- Burack MA, Hartlein J, Flores HP, Taylor-Reinwald L, Perlmutter JS, Cairns NJ. In vivo amyloid imaging in autopsy-confirmed Parkinson disease with dementia. *Neurology*. 2010;74:77–84.
- Morris JC, Roe CM, Xiong C, et al. APOE predicts A β but not tau Alzheimer's pathology in cognitively normal aging. *Ann Neurol*. 2010;67:122–131.